



THE UNIVERSITY *of* EDINBURGH

Edinburgh Research Explorer

A novel Franchot engine design based on the balanced compounding method

Citation for published version:

Daoud, J & Friedrich, D 2018, 'A novel Franchot engine design based on the balanced compounding method' Energy Conversion and Management.

Link:

[Link to publication record in Edinburgh Research Explorer](#)

Document Version:

Peer reviewed version

Published In:

Energy Conversion and Management

General rights

Copyright for the publications made accessible via the Edinburgh Research Explorer is retained by the author(s) and / or other copyright owners and it is a condition of accessing these publications that users recognise and abide by the legal requirements associated with these rights.

Take down policy

The University of Edinburgh has made every reasonable effort to ensure that Edinburgh Research Explorer content complies with UK legislation. If you believe that the public display of this file breaches copyright please contact openaccess@ed.ac.uk providing details, and we will remove access to the work immediately and investigate your claim.



1 A novel Franchot engine design based on the balanced compounding method

2 Jafar M. Daoud, Daniel Friedrich*

3 *School of Engineering, Institute for Energy Systems, University of Edinburgh, EH9 3DW (Scotland)*

4 *Corresponding author Email: d.friedrich@ed.ac.uk

5 **Abstract:** *The Franchot engine is a double acting Stirling engine with only two cylinders and freely controllable*
6 *phase angle. The hot and cold cylinders of the Franchot engine can be directly heated and cooled and thus act as*
7 *heaters/coolers. However, the cylinders are necessarily long and thin to increase the heat transfer area and hence*
8 *the power. The long strokes result in long cranks and connecting rods which lead to large and unwieldy engines.*
9 *In this contribution, the directly heated and cooled multi-cylinder Franchot engine is dynamically studied with a*
10 *novel balanced compounding mechanism. Thus, the balanced compound Franchot engine would be more*
11 *compact, cheaper and more efficient due to the removal of the rotational parts. The new mechanism includes a*
12 *linkage between two connecting rods in a conventional Franchot engine for which, four pistons (an expansion,*
13 *compression and two guiding pistons) move as one reciprocator. The influence of different engine parameters,*
14 *such as number of cylinders, temperature, dead volume and reciprocator mass, on the new configuration is*
15 *investigated. The possible phase angles for each number of cylinders are given. The balanced compound Franchot*
16 *engine changes the order of piston motion so that the largest of these phase angles is obtained. The theoretical*
17 *analysis shows that increasing the number of cylinders, dead volume and reciprocating mass reduces the*
18 *frequency and increases the stroke; increasing the cylinder diameter increases the frequency and decreases the*
19 *stroke; increasing the load decreases the stroke and slightly decreases the frequency; and increasing the*
20 *temperature increases both the frequency and the stroke. Thus, different engine parameters can be used to*
21 *maximise the power generation without the piston hitting the cylinder head. The dynamic load, which is a*
22 *function of the speed, does not prevent the balanced compound Franchot engine from self-starting while static*
23 *friction can prevent the engine from self-starting, especially if the pistons are around the mid-stroke point. The*
24 *most promising configuration is the three-phase engine which has the lowest number of cylinders, preferable*
25 *phase angle and phase shift of 120° and potential for electricity generation and heat pumping.*

26 **Keywords:** *Franchot engine; Stirling engine; multi-cylinder; phase angle; phase shift; balanced compounding*

27 1 Introduction

28 The Franchot engine which is a double acting Stirling engine was invented in the 19th century by
29 Charles Louis Franchot [1]. The design of Stirling engines, which is a compromise between power and
30 thermal efficiency, is still an open and widely studied problem [2][3][4]. In the Franchot engine, only
31 two pistons are required, the phase angle can be freely controlled and each cylinder is either hot or
32 cold which eliminates the shuttle and axial conduction losses [5]. Double acting as well as single acting
33 Stirling engines can use the simple slider crank drive [6][7]. Kinematic drives convert the reciprocal
34 motion into rotational motion and mechanically fix the relation between engine parameters, such as
35 the phase angle, phase shift and stroke length. However, kinematic Stirling engines were not cost
36 effective, mechanically reliable or mass produced [8][9]. The free piston concept offers a linear driving
37 mechanism without a need for a rotational cranking mechanism. The free piston concept can be used
38 in applications for which the linear motion can be directly used, e.g. linear electricity generator, liquid
39 pump, gas compressor or heat pump [10].

40 The free piston Stirling engine (FPSE) was introduced by Beale in 1969 and patented in 1972 for single
41 acting engines which have the crankshaft replaced by gas or mechanical springs [11][12]. The force
42 that is needed to complete the compression stroke is stored in the spring instead of being transferred
43 through the crankshaft. The absence of the crankshaft results in the removal of the rotating parts,
44 lubrication system, support structure and connecting rods. This implies that the FPSE has small side

45 thrust forces, excellent thermal efficiency, reduced mechanical wear and can be hermetically sealed
46 which makes it compacter, more reliable and cheaper than conventional engines [11]. However, the
47 FPSE experiences variations of the stroke length and phase angle as a response to the load and has
48 hysteresis losses due to the internal friction of the springs which is dissipated as heat [8][13][14]. The
49 FPSE might experience over strokes that cause the power piston to strike the cylinder ends [15][16].
50 Hence, auxiliary devices are needed to limit the stroke. The free piston concept can be extended to
51 the multi-cylinder Siemens configuration where higher power density and a lower number of moving
52 parts and springs are obtained. The reliability of the multi-cylinder FPSE can be increased if the pistons
53 are replaced by membranes hence, mechanical friction can be avoided and sealing becomes much
54 easier [9].

55 It has been reported that, at least three cylinders are needed to achieve the multi-cylinder Siemens
56 engine [7][9][17]. Unlike the single acting engine where the phase angle is a function of spring
57 stiffness, the multi-cylinder engine has its phase angle and phase shift governed by the number of
58 cylinders. For each cylinder thermodynamically connected to an adjacent cylinder, the phase angle
59 which defines the lag between hot and cold spaces can be represented as a function of the number N
60 of cylinder as $\theta = 180^\circ - \frac{360^\circ}{N}$ [18]. The phase shift which determines the sequence of the
61 reciprocating pistons is given by $\theta_s = \frac{360^\circ}{N}$ [19].

62 For any Stirling machine the preferred phase shift is within the range 90° - 140° [20]. Only the three and
63 four cylinder Siemens configurations fall into this range. At the highly preferable phase shift 120°
64 which can be obtained from the 3 cylinder engine, a non-recommended phase angle equal to 60° is
65 obtained which increases the fractional volumetric variation hence contributes in increasing the
66 hysteresis losses [21].

67 A liquid piston engine (also known as Fluidyne) was invented by Colin D. West in 1969 [22]. In liquid
68 piston engines, the mechanical pistons and connecting rods are replaced by liquid columns and the
69 coupling forces in the FPSE are replaced by the hydrodynamic and hydrostatic forces [23]. In multi-
70 cylinder liquid piston engines such as the Siemens configuration, each hot to cold space shares the
71 same liquid column so that they are coupled pneumatically and hydraulically which defines the phase
72 angle.

73 In 1978, Finkelstein [24] presented a novel coupling mechanism called the balanced compounding of
74 Stirling machines for which he was granted a patent in 1980 [25]. Instead of storing some of the
75 expansion energy in a rotating crankshaft, springs or hydrostatic columns for the compression stroke,
76 an opposite engine group is added. Both engine groups are coupled mechanically through straight
77 connecting rods. Thus, in this arrangement each connecting rod connects two cylinders. Hence, an
78 even number of double acting Stirling machines is required. In the Finkelstein configuration, the
79 connecting rods are located to the cold cylinder side and can be as short as possible due to the absence
80 of heat transfer between the facing parts. By rearranging the engine compartment, a balanced
81 compound 4 cylinder engine where each cylinder is either hot or cold can be obtained. This becomes
82 a dual Franchot engine which eliminates heat conduction and shuttle losses but has heat transfer
83 losses due to the connecting rod. In this configuration, the Franchot engines generate opposite forces
84 as it comprise two opposite alpha type Stirling engine. Hot spaces are both gas and mechanically
85 coupled to the cold spaces by the regenerators and connecting rods, respectively. However, to keep
86 the phase angle advanced by 90° for all of the four hot spaces, half the regenerator connections are
87 longer and have to cross.

88 Finkelstein showed in his patent many variations of the FPSE based on the balanced compounding
89 technique. For example, a one-cylinder engine in which different work volumes are coupled
90 mechanically using two concentric shafts can be equivalent to the 4-cylinder engine. Similar to the
91 FPSE, this mechanism comprise the lowest possible side forces, absence of rotating parts, hence,
92 increased seal life, improved engine performance and ability to hermitically seal engine
93 compartments.

94 The balanced compound engine was investigated based on the phasor diagram and ideal Schmidt
95 analysis of the isothermal Stirling engine [24]. The analysis shows that the proposed engine can
96 generate net positive power. Finkelstein [26] obtained an analytical solution for the balanced
97 compounding Vuilleumier cycle with two hot, two warm and two cold cylinders which require 8
98 regenerators with long connections, six hot heat exchangers and two connecting rods. His model is
99 based on ideal assumptions, isothermal expansion and compression processes and only works with
100 FPSE. The analytical solution showed that the piston oscillation is sinusoidal and the phase shift is 90° .
101 In 1992, Finkelstein [27] analysed the balanced compound Vuilleumier heat pump using a simpler
102 model based on the sinusoidal variations of the swept volumes. The new model showed negligible
103 differences with the FPSE model. The new model can be used for both the kinematic and free piston
104 machines. However, no experimental study or real machine was reported to be manufactured.

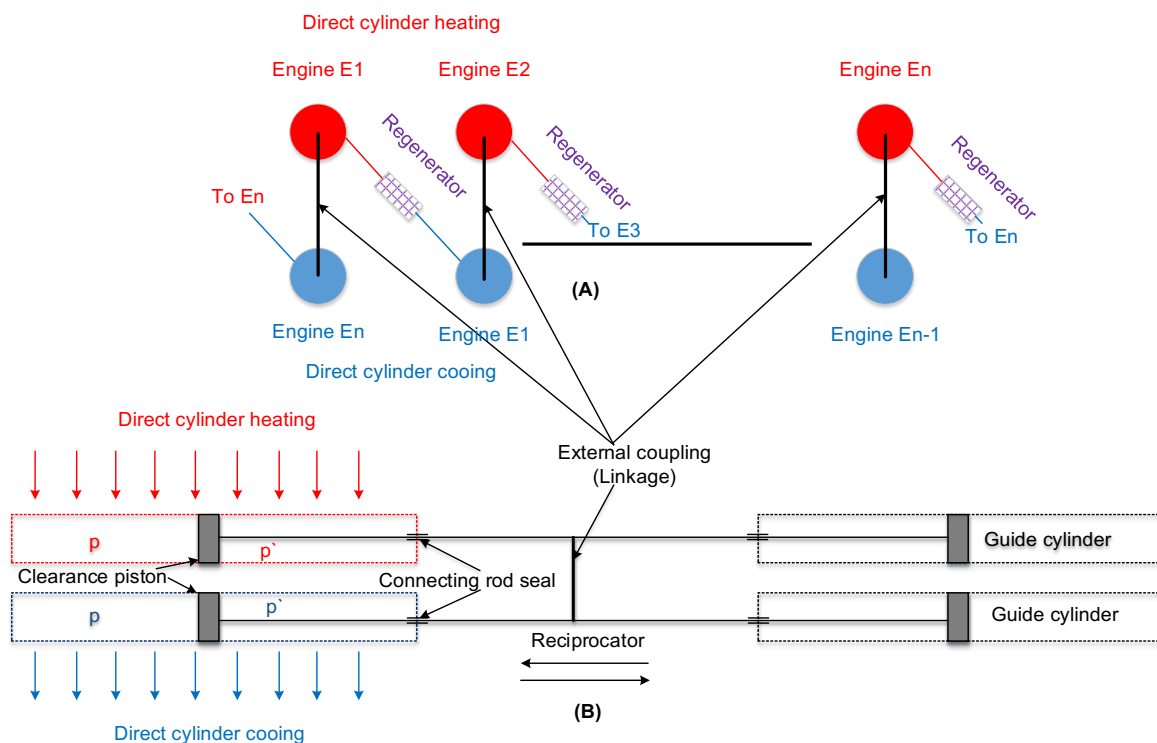
105 McConaghy [28] patented a new arrangement for 3-phase AC power generation which is composed
106 from two 3-ph gamma type engines working opposite to each other and coupled electrically. Each
107 cylinder has a piston and a displacer rigidly coupled by a rod. This design makes it possible to get rid
108 of the connecting rods between different cylinders and to hermetically seal all engine compartments
109 but it still has a bounce volume, displacers and double the number of sliding objects. In addition to
110 that, the operation is dependent on the load. In 2014, Dadd [29] patented a linear multi-cylinder
111 Stirling machine. In this machine, the hot and cold volumes are coupled by gas and common
112 connecting rods. This machine has the same number of connecting rods and cylinders but uses the
113 linear power transmitters such as linear motors and generators as coupling mechanism.

114 In our previous work [30][31], we introduced, modelled and investigated the cylinder heated and
115 cooled Franchot engine and developed a novel isothermaliser design to improve the power density.
116 However, the engine still uses long cylinders to enhance the heat transfer and power generation. Long
117 cylinders require long cranks which leads to a long engine, piston side forces and vibrations. A multi-
118 cylinder configuration can enhance power generation and reduce the vibrations for the simple slider
119 crank mechanism [32]. Nevertheless, rotational parts are responsible for increasing the complexity,
120 unreliability, losses and cost. The use of gas or mechanical spring coupling might not be the suitable
121 option for the cylinder heated and cooled engine. Long bounce spaces or long mechanical springs can
122 generate large losses in addition to increasing the engine length. The directly heated and cooled
123 Franchot engine cannot also use the balanced compounding innovated by Finkelstein due to long
124 regenerator connections. Moreover, the opposite engines configuration requires only an even pair of
125 hot cylinders and results in distributed heaters and coolers.

126 In this study, the slider crank mechanism is replaced by a novel driving method based on the balanced
127 compounding principle. We extend our previous works to evaluate the impact of using the balanced
128 compounding principle on the mechanical engine performance. In addition to the potential power
129 improvements, this study investigates the potential of the engine to self-start. A tailored mathematical
130 model for the balanced compound Franchot engine is derived which is suitable for an arbitrary number
131 of cylinders.

132 **2 Balanced compounding of the cylinder heated/cooled Franchot engine**

133 Here, the side-by-side balanced compound arrangement is suggested which has reduced regenerator
 134 connection lengths and directly cooled and heated cylinders. It requires a minimum of three phases
 135 to make a multiple Franchot engine with straight and short regenerator connections. The top and side
 136 view for the balanced compound directly heated and cooled $n - ph$ engine are shown in Figure 1.
 137 Each cold cylinder is coupled with a conjugate hot cylinder mechanically via an external crank and
 138 through the regenerator to the corresponding hot cylinder of the engine. Each crank connects two
 139 Franchot engines and each Franchot engine is connected to two cranks according to the ordering
 140 shown. Only one long but straight regenerator connection is needed in the engine En which can be
 141 shortened by a round topology. Each compression piston can move parallel to an expansion piston at a
 142 predefined phase angle. The compression work will be compensated by the expansion work without
 143 a crankshaft and flywheel [24]. However, the zero side forces obtained by the Finkelstein arrangement
 144 are not achievable by this configuration. The side forces in this arrangement are expected to be
 145 smaller than the forces of the slider crank engine due to the shorter crank length. The crank length in
 146 the kinematic engine is half of the stroke length while the crank length in the balanced compound
 147 engine can be much shorter based on the required distance between the cylinders such as the need
 148 to add thermal insulators or mountings.



149

150 *Figure 1: Balanced compounding of the multi-cylinder Franchot engine. A) cross sectional view showing the n-phase engine*
 151 *and B) side view showing two cylinders of the multi-cylinder configuration.*

152 In the kinematic engine, the phase angle of the multi-cylinder Franchot engine can be predicted based
 153 on the regenerator connection as shown in Table 1 [32][33]. In the balanced compounding, the
 154 regenerator connection is determined by the order of piston motion. It is expected that the balanced
 155 compound engine will work on one of the listed angles. However, Berchowicz and Kwon [20]
 156 anticipated the phase angle will decrease for increasing the number of cylinders of the stepped piston
 157 design.

158

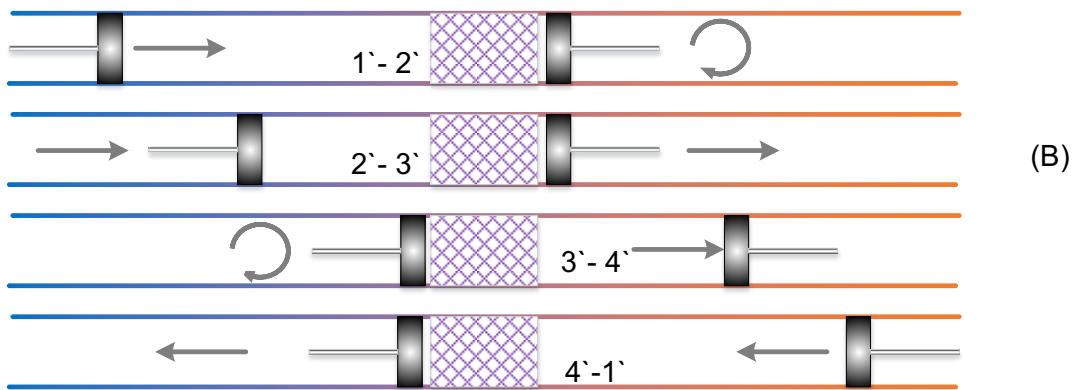
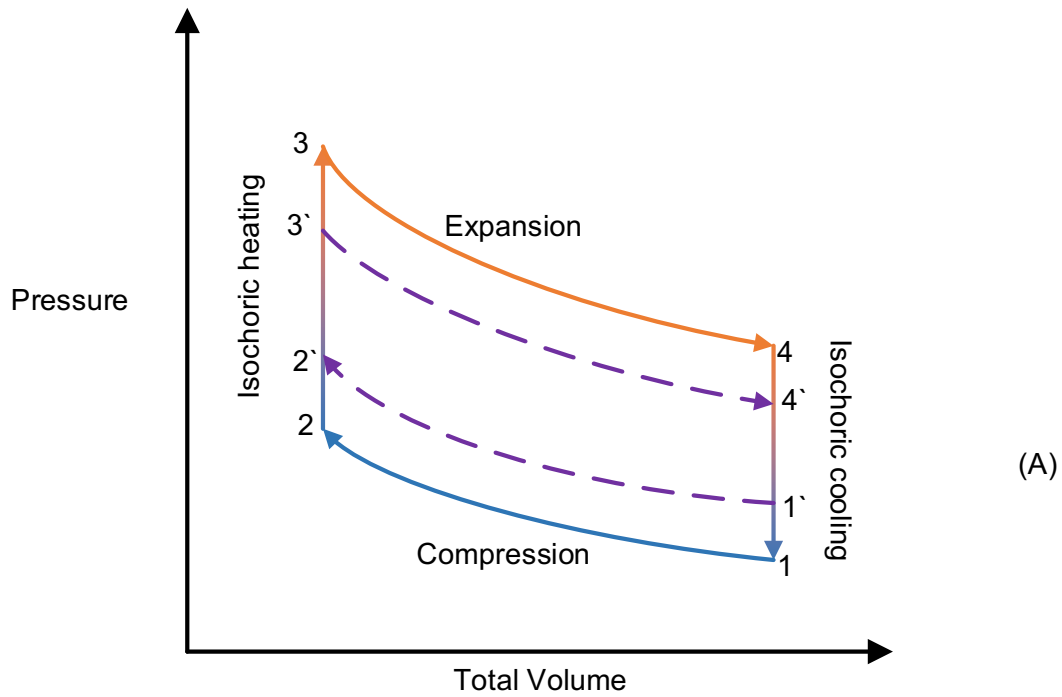
Table 1: Possible phase angles of the multi-cylinder Franchot engine for different numbers of cylinders

	3-ph	4-ph	5-ph	6-ph	7-ph	8-ph
y=2	120°	90°	72°	60°	51.4°	45°
y=4			144°	120°	102.8°	90°
y=6					154.2°	135°

159

160 Figure 2 shows the thermodynamic cycle of a Stirling engine having two opposite pistons. The
 161 expansion piston always leads the compression piston by an arbitrary phase angle. The direct cylinder
 162 heated and cooled Stirling engine comprises two polytropic and two isochoric processes according to
 163 piston motion from 1`-4`. The ideal engine has isothermal instead of the polytropic processes for the
 164 piston motion from 1-4, though.

- 165 • 1`-2` Polytropic compression: In this process, the expansion piston stands still and the
 166 compression piston moves inward. The heat is rejected alongside the walls of the cold cylinder
 167 corresponding to the working space due to the gas temperature difference with the cold
 168 cylinder walls. The engine requires some work in order to compress the working fluid and the
 169 pressure increases.
- 170 • 2`-3` Isochoric heating: In this process, the expansion and compression pistons move outward
 171 and inward, respectively. They move against each other and keep the total volume of the
 172 working spaces constant. The gas flows from the compression to the expansion space and
 173 passes through the regenerator which absorbs heat from it. In this process, the pressure of
 174 the gas increases and no work is required or generated since there is no change in the total
 175 engine volume.
- 176 • 3`-4` Polytropic expansion: In this process, the compression piston stands still and the
 177 expansion piston moves outward. Energy is absorbed alongside the wall of the hot cylinder
 178 corresponding to the hot working space due to the temperature difference between the hot
 179 cylinder walls and working gas. The cycle generates positive work and the gas pressure
 180 decreases.
- 181 • 4`-1` Isochoric cooling: In this process, the expansion piston moves inward and the
 182 compression piston moves outward . Both move against each other keeping the total volume
 183 of the working spaces constant. The gas flows from the expansion to the compression space
 184 through the regenerator. The gas re-absorbs the heat which was absorbed in step 2`-3` into
 185 the regenerator. In this process, no mechanical work is required or generated since there is
 186 no change in the total engine volume and the working gas pressure decreases.

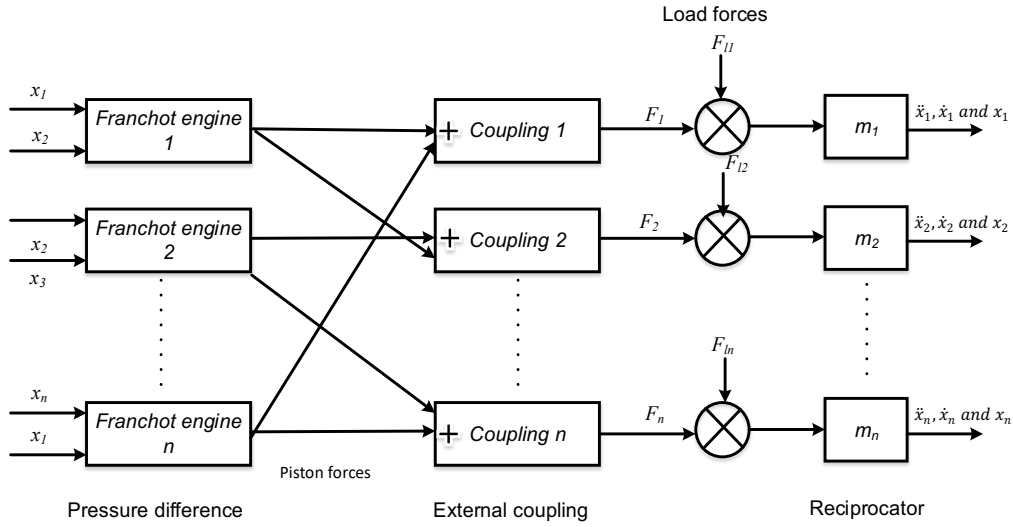


187

188 *Figure 2: Thermodynamic cycle of the Stirling engine: A) PV diagram of the ideal (1-2-3-4) and polytropic (1'-2'-3'-4') cycle*
 189 *and B) piston displacements for the polytropic cycle.*

190 **3 Methodology**

191 Figure 3 shows the relationship between the forces, reciprocators and displacement of each
 192 component of the balanced $n - ph$ Franchot engine. The $n - ph$ Franchot engine is composed from
 193 $2 * n$ alpha type Stirling engines. In which, each alpha type Stirling engine is modelled separately.



194

195 *Figure 3: Schematic diagram of the $n - ph$ balanced compound Franchot engine which shows the forces and nomenclature.*

196 Applying Newton's second law of motion, the force balance equation implies

$$\begin{bmatrix} F_1 \\ F_2 \\ \vdots \\ F_n \end{bmatrix} = \begin{bmatrix} m_1 \\ m_2 \\ \vdots \\ m_n \end{bmatrix} [\ddot{x}_1 \quad \ddot{x}_2 \quad \dots \quad \ddot{x}_n] + \begin{bmatrix} F_{l1} \\ F_{l2} \\ \vdots \\ F_{ln} \end{bmatrix} \quad 1$$

197

198 where F is the thermal driving force, m is the total mass of reciprocating elements as a bulk, F_l is the
199 load force, x is the reciprocator displacement.

200 The power is calculated for the $n - ph$ Franchot engine as follows

$$P = F_1 \dot{x}_1 + F_2 \dot{x}_2 + \dots + F_n \dot{x}_n \quad 2$$

201

202 The thermal forces applied to each connecting rod are calculated from

$$\begin{bmatrix} F_1 \\ F_2 \\ \vdots \\ F_n \end{bmatrix} = \begin{bmatrix} \Delta p_{E1} & \Delta p_{En} \\ \Delta p_{E2} & \Delta p_{E1} \\ \vdots & \vdots \\ \Delta p_{En} & \Delta p_{En-1} \end{bmatrix} \begin{bmatrix} A_{h1} & A_{h2} & \dots & A_{hn} \\ A_{kn} & A_{k1} & \dots & A_{kn-1} \end{bmatrix} \quad 3$$

203

204 where A_h and A_k are the cross sectional area of the hot and cold pistons respectively, Δp is the
205 pressure difference across the pistons of the Franchot engine, F_l is the force due to the load and the
206 subscript E denotes the Franchot engine.

207 If all reciprocators have the same cross sectional area and mass then the acceleration of the pistons
208 can be calculated by rearranging the fore balance equation and the thermal forces to get the following
209 equation:

$$\begin{bmatrix} \ddot{x}_1 \\ \ddot{x}_2 \\ \vdots \\ \ddot{x}_n \end{bmatrix} = \frac{A}{m} \left(\begin{bmatrix} \Delta p_{E1} + \Delta p_{En} \\ \Delta p_{E2} + \Delta p_{E1} \\ \vdots \\ \Delta p_{En} + \Delta p_{En-1} \end{bmatrix} - \begin{bmatrix} F_{l1} \\ F_{l2} \\ \vdots \\ F_{ln} \end{bmatrix} \right) \quad 4$$

210

211 The speed and displacement of the pistons are calculated by calculating the integral and double
 212 integral of the acceleration matrix, respectively.

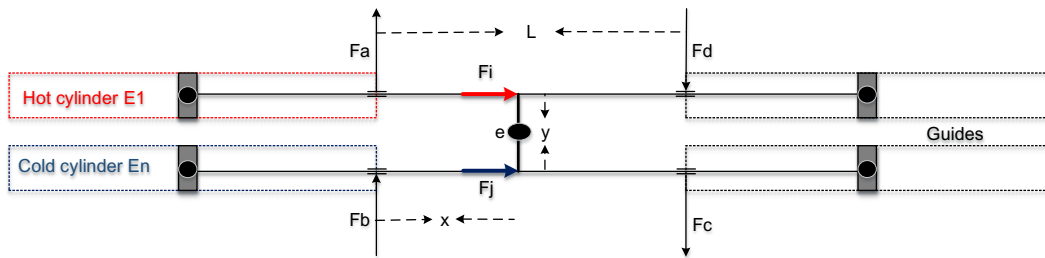
213 The free piston Stirling engine is considered a mass damper system where the generic load acting on
 214 its moving pistons can be approximated by a damping load in which the load force is written as
 215 [10][13][34][35]:

$$\begin{bmatrix} F_{l1} \\ F_{l2} \\ \vdots \\ F_{ln} \end{bmatrix} = \begin{bmatrix} c_1 \\ c_2 \\ \vdots \\ c_n \end{bmatrix} [\dot{x}_1 \quad \dot{x}_2 \quad \dots \quad \dot{x}_n] \quad 5$$

216

217 where c is the damping coefficient.

218 The friction is another type of load that reduces the Stirling engine performance and needs to be
 219 reduced. For sliding pistons the coefficient of friction is around 0.2 [36]. There are two mechanical
 220 friction sources in this configuration; the friction due to the weight of the reciprocating masses and
 221 the friction due to the side forces created by the cylinder offset. The side forces can be obtained by
 222 analysing the free body diagram of the engine as shown in Figure 4. The analysis considers the worst
 223 case when the rod sleeves are tight enough to handle all mechanical friction. Besides their roll to guide
 224 the connecting rods, guiding cylinders can be used as additional engine to serve as a load like heat
 225 pump or fluid pump.



226

227 *Figure 4: Free body diagram of the balanced compound Franchot engine.*

228 Taking the moment of inertia around the non-rotating point e applies:

$$\sum M_e = 0 \quad 6$$

229 hence,

$$\frac{y}{2}(F_j - F_i) - x(F_a + F_b) - (L - x)(F_c + F_d) = 0 \quad 7$$

230 As the connecting rod is only free to move along the cylinder axis (x) then

$$\sum F_y = 0 \quad 8$$

231 This implies that

$$F_a + F_b = F_c + F_d \quad 9$$

232 hence, the total side force can be calculated as:

$$F_a + F_b + F_c + F_d = \frac{y * (F_j - F_i)}{L} = \frac{y}{L} \Delta F \quad 10$$

233 where,

$$\Delta F = \begin{bmatrix} \Delta F_1 \\ \Delta F_2 \\ \vdots \\ \Delta F_n \end{bmatrix} = A \begin{bmatrix} \Delta p_{E_n} - \Delta p_{E_1} \\ \Delta p_{E_1} - \Delta p_{E_2} \\ \vdots \\ \Delta p_{E_{n-1}} - \Delta p_{E_n} \end{bmatrix} \quad 11$$

234

235 The load force due to the mechanical friction can be written as:

$$\begin{bmatrix} F_{l1} \\ F_{l2} \\ \vdots \\ F_{ln} \end{bmatrix} = \begin{bmatrix} \left\{ \begin{array}{l} 0.2(m_1g + |\Delta F_1|) \\ -0.2(m_1g + |\Delta F_1|) \end{array} \right\} & \left\{ \begin{array}{l} \dot{x}_1 < 0 \\ \dot{x}_1 > 0 \end{array} \right\} \\ \left\{ \begin{array}{l} 0.2(m_2g + |\Delta F_2|) \\ -0.2(m_2g + |\Delta F_2|) \end{array} \right\} & \left\{ \begin{array}{l} \dot{x}_2 < 0 \\ \dot{x}_2 > 0 \end{array} \right\} \\ \vdots & \vdots \\ \left\{ \begin{array}{l} 0.2(m_ng + |\Delta F_n|) \\ -0.2(m_ng + |\Delta F_n|) \end{array} \right\} & \left\{ \begin{array}{l} \dot{x}_n < 0 \\ \dot{x}_n > 0 \end{array} \right\} \end{bmatrix} \quad 12$$

236

237 The resonant frequency of the free piston Stirling engine is a function of the reciprocating mass and
238 spring stiffness as [37][19]:

$$\omega_o = \sqrt{\frac{k}{m}} \quad 13$$

239 The spring stiffness of the balanced compound Franchot engine which is pressure coupled can be
240 calculated from the stiffness of the working gas. The working gas stiffness has a maximum value if the
241 expansion and compression processes are adiabatic which is given by [21]:

$$k = \frac{\gamma p A^2}{V} \quad 14$$

242 The stiffness has a minimum value if the expansion and compression processes are isothermal which
243 is given by [21]:

$$k = \frac{p A^2}{V} \quad 15$$

244 Since the expansion and compression processes are polytropic then the working gas stiffness can be
245 written as:

$$k = \frac{np A^2}{V} \quad 16$$

246 where n is the polytropic index which can be calculated from [38] as:

$$n = -\frac{V dp}{p dv} \quad 17$$

247 Applying the mass balance equation on the engine 3 control volume yields in [30]

$$m = m_e + m_c + m_r \quad 18$$

248 Deriving the mass balance equation gives

$$\dot{m} = \dot{m}_e + \dot{m}_c + \dot{m}_r \quad 19$$

249 The mass leakage in this engine is the summation of the leakage on the hot and cold pistons and is
250 written as

$$\dot{m} = \dot{m}_{le} + \dot{m}_{lc} \quad 20$$

251 The energy balance equation of the expansion volume can be written by considering the gas leakage
 252 at the expansion piston as follows

$$\dot{Q}_e + \dot{H}_e + c_p \dot{m}_e T_{re} = p \dot{v}_e + c_v (\dot{m}_e T_e) \quad 21$$

253 By rearranging equation 21, the mass flow rate in the expansion chamber results in

$$\dot{m}_e = \frac{\frac{p \dot{v}_e}{R} + \frac{v_e \dot{p}}{\gamma R} - \frac{\dot{Q}_e + \dot{H}_e}{c_p}}{T_{re}} \quad 22$$

254 Similarly, the mass flow rate in the compression chamber is written as

$$\dot{m}_c = \frac{\frac{p \dot{v}_c}{R} + \frac{v_c \dot{p}}{\gamma R} - \frac{\dot{Q}_c + \dot{H}_c}{c_p}}{T_{cr}} \quad 23$$

255 The regenerator mass flow rate is calculated from

$$\dot{m}_r = \frac{V_r}{RT_r} \dot{p} \quad 24$$

256 The differential form of the pressure obtained by combining Equations 19, 22, 23 and 24 becomes

$$\dot{p} = \frac{-p \left(\frac{\dot{v}_e}{T_{re}} + \frac{\dot{v}_c}{T_{cr}} \right) + \frac{R}{c_p} \left(\frac{\dot{Q}_e + \dot{H}_e}{T_{re}} + \frac{\dot{Q}_c + \dot{H}_c}{T_{cr}} \right) + R \dot{m}}{\frac{v_e}{\gamma T_{re}} + \frac{V_r}{T_r} + \frac{v_c}{\gamma T_{cr}}} \quad 25$$

257 where v , T , \dot{Q} , \dot{H} and m denote the volume, temperature, heat flow rate, enthalpy and mass leakage
 258 in the working spaces, respectively and subscripts e , r and c indicate the expansion, regeneration and
 259 compression space, respectively.

260 The Franchot engine enjoys small enthalpy loss as the leaks shuttle between similar temperature
 261 chambers. The enthalpy is calculated as [39]

$$\dot{H} = c_p \dot{m}_l T \quad 26$$

262 where T depends on the mass leakage direction between opposite expansion or compression spaces.
 263 It is the source temperature for positive mass flow rate and working space temperature for negative
 264 mass flow rate.

265 The mass leakage through a clearance seal where the flow is laminar is calculated from [7][39]

$$\dot{m}_l = \pi D \frac{p + \dot{p}}{4RT_g} \left(\dot{x} \delta - \frac{\delta^3}{6\mu} \frac{p - \dot{p}}{L_g} \right) \quad 27$$

266 where p , \dot{p} , T_g , \dot{x} , δ , μ and L_g are instantaneous pressure, pressure at opposite chamber, gas
 267 temperature, linear piston velocity, piston to cylinder wall gap, dynamic viscosity and gap length.

268 Regenerator end temperatures are calculated from [30]:

$$T_{rh} = \frac{-\phi i \dot{m}_e T_e}{\phi (1 - i) \dot{m}_e} \quad 28$$

269

$$T_{rk} = \frac{-\phi j \dot{m}_c T_c}{\phi (1 - j) \dot{m}_c} \quad 29$$

270 where the parameters i and j are given by

$$i = \begin{cases} 1, & \dot{m}_e < 0 \\ 0, & \dot{m}_e \geq 0 \end{cases} \quad 30$$

$$j = \begin{cases} 1, & \dot{m}_c < 0 \\ 0, & \dot{m}_c \geq 0 \end{cases} \quad 31$$

271

272 Hence, the average regenerator temperature is:

$$T_r = \frac{T_{rh} - T_{rk}}{\ln \frac{T_{rh}}{T_{rk}}} \quad 32$$

273 External irreversibility is considered through the heat addition and removal which are calculated from
274 Newton's law of cooling [40]:

$$\dot{Q} = hA\Delta T \quad 33$$

275

276 where h is the convective heat transfer coefficient, which holds for Reynolds' numbers between 1000
277 and 100,000 and is calculated as [41]:

$$h_e = 0.042D_h^{-0.42}v^{0.58}p^{0.58}T^{-0.19}$$

$$h_c = 0.0236D_h^{-0.47}v^{0.53}p^{0.53}T^{-0.11} \quad 34$$

278

279 where ΔT , D_h , h_e and h_c are the temperature difference between the working gas and cylinder wall,
280 hydraulic diameter, convective heat transfer during the expansion and compression, respectively.

281 4 Results and discussion

282 The model is implemented in Matlab/Simulink and solved using the Runga-Kutta method with a time
283 step of 10^{-4} s. All results use the reference engine parameters listed in Table 2 unless otherwise stated.
284 The reference engine is considered ideal and the mechanical Friction and regenerator pumping losses
285 are considered as friction and damping load, respectively.

286

Table 2: Parameters of the reference engine

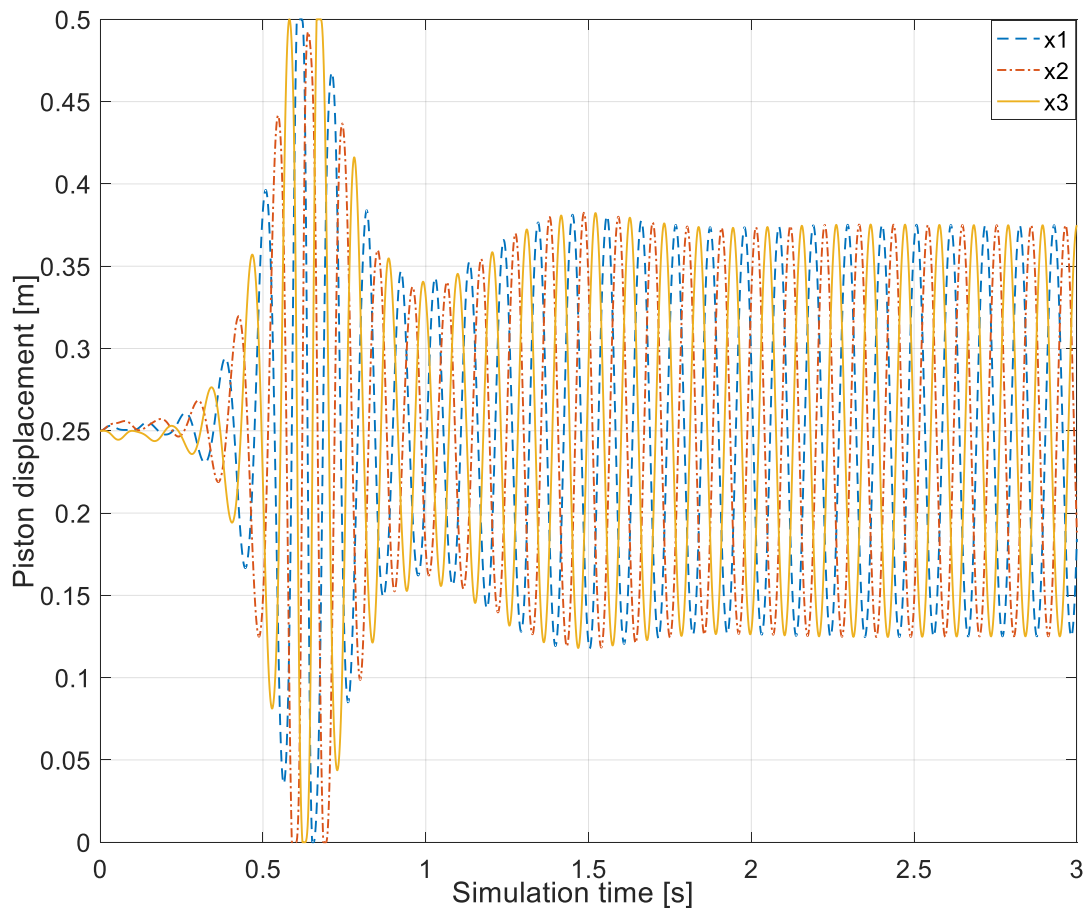
Name	symbol	value/unit
Stroke length	L_e, L_c	50 cm
Bore diameter	D_e, D_c	2.5 cm
Gas density	ρ	1.225 kg/m ³
Reciprocator mass	m	0.1 kg
Reg. volume	V_r	0 cm ³
Number of phases	n	3
Temperatures	T_h, T_k	450 K, 300 K
Link length	y	4 cm
Working gas	Air	
Gas constant	R	287 J/kg.K

287

288 **4.1 Effect of friction**

289 The start-up of the balanced compound engine is highly dependent on the static friction. Figure 5
290 shows the dynamic response of the 3-ph balanced compound Franchot engine in which, a minimum
291 pressure difference of 3.67 kN/m² is needed to aid start-up. The force generated by this difference
292 overcomes the static friction which is caused by the side forces and weight of the reciprocator. In a
293 real application, pistons must be shifted from mid-stroke point so that a pressure difference can
294 develop. Otherwise, an external starter might be required. However, it is very unlikely that all pistons
295 stop exactly at the mid-stroke. The friction which is responsible for starting problems aids braking the
296 balance at stopping stage especially when engine temperature difference is getting reduced. The mid-
297 stroke equilibrium point may be affected by the difference in the regenerator volumes or the
298 reduction of the swept volume due to the connecting rod. Unlike the balanced compound engine, the
299 kinematic engine has the stroke, phase angle, phase shift and the instantaneous position of pistons
300 predefined. Hence, pressure variations occur once the engine is heated which cause the kinematic
301 engine to start-up regardless of the crank angle.

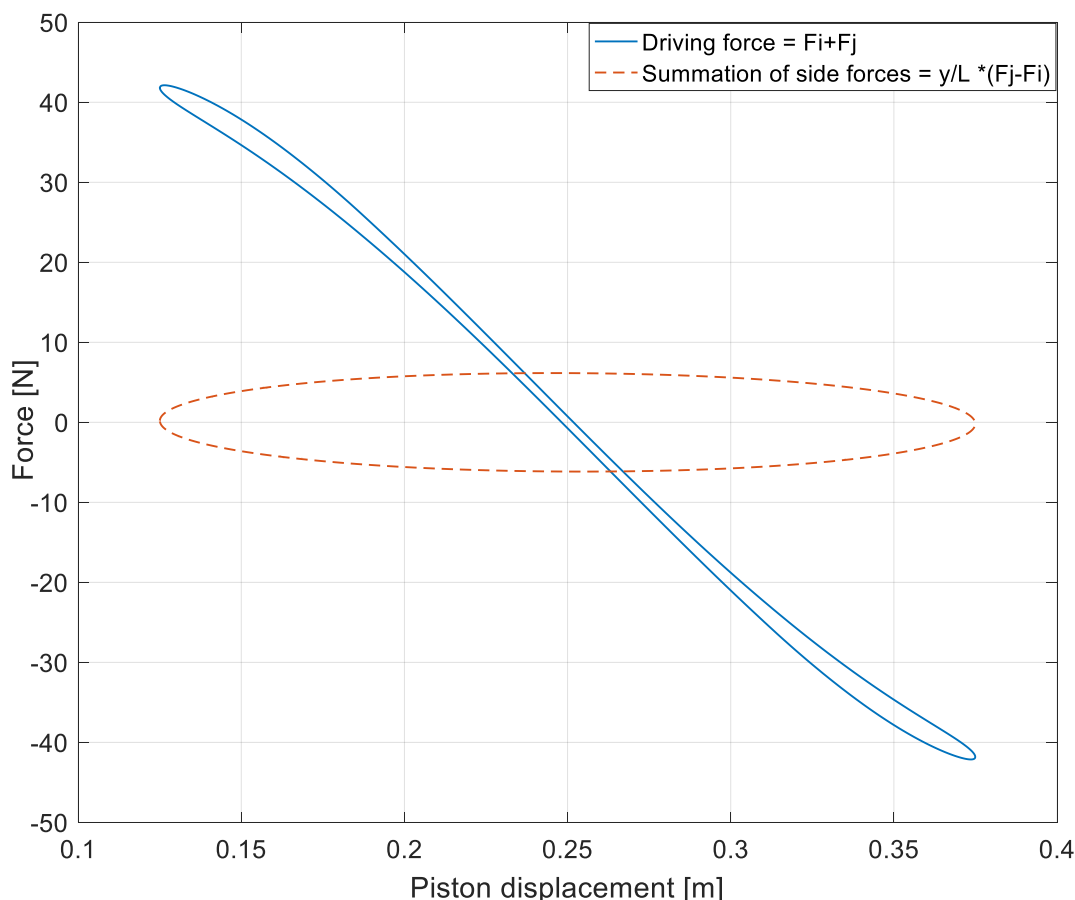
302 The dynamic response shows that the volume and phase angles are exactly 120° degree. Different
303 angles are less likely to happen due to the anticipated negative power which hinders the piston
304 motion. At the steady state, piston displacements are symmetric and can be represented by sinusoidal
305 functions [27].



306
307 *Figure 5: No-load dynamic start-up response of the reference 3-ph Franchot engine considering the mechanical friction.*

308 The driving force and the side force due to the eccentricity of the new cranking mechanism are shown
309 in Figure 6. The maximum driving force occurs at the full stroke while the side forces are minimum

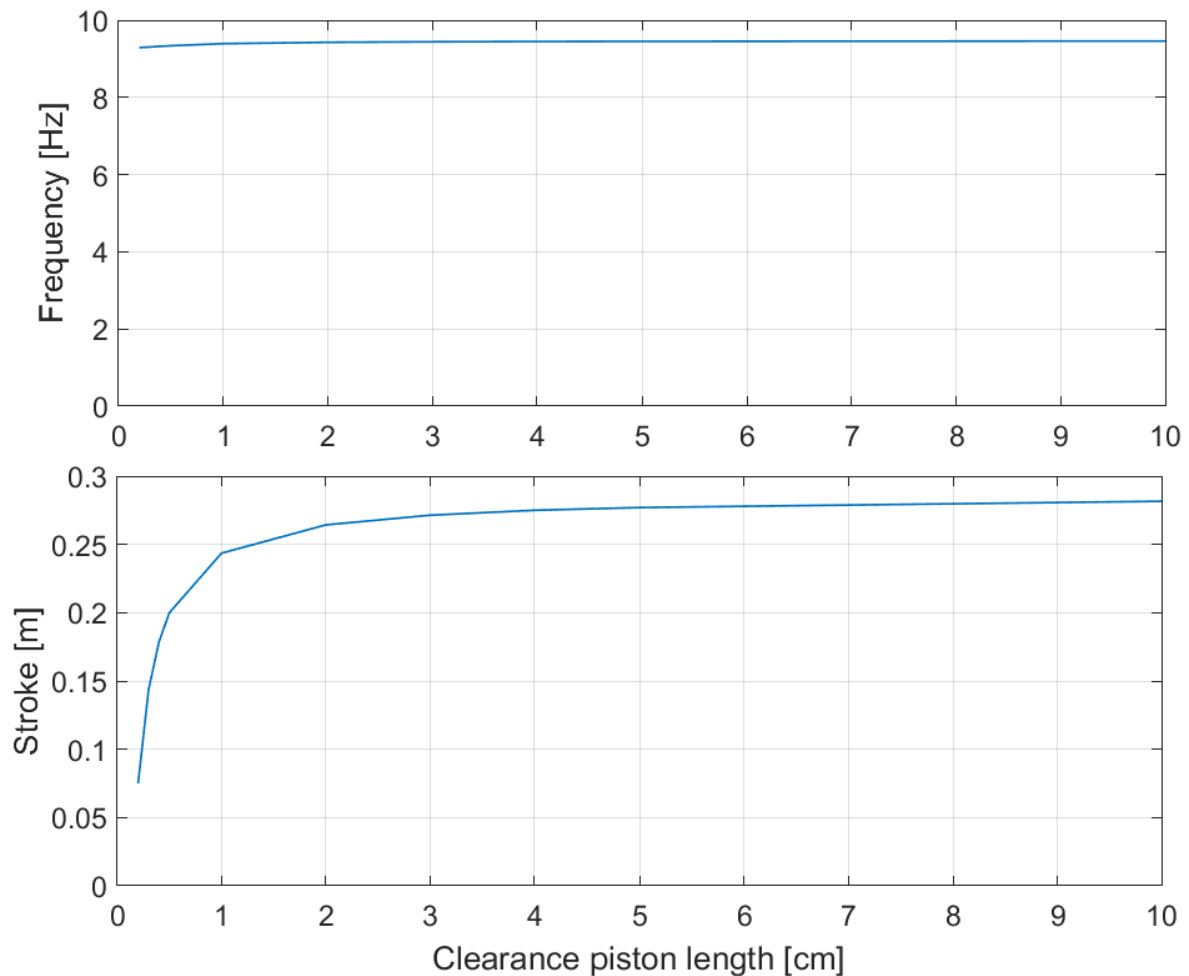
310 hence maximum acceleration occurs. The worst case occurs around mid-stroke where the largest side
 311 forces and smallest driving force exist. However, at mid-stroke the kinetic energy is maximum and acts
 312 similar to the flywheel to overcome negative loads such as friction or speed dependant loads.



313
 314 *Figure 6: Loading forces of the new cranking mechanism.*

315 **4.2 Effect of gas leakage**

316 In Stirling engines, gas leakage must be prevented in order to achieve the design performance.
 317 Different methods are used to overcome gas leakage such as using pressurised crankcase, tight seals,
 318 diaphragm pistons, liquid pistons and gas compensation. In this study, tight clearance seals are being
 319 suggested. The gas leakage due to the clearance of the connecting rod is not considered due to the
 320 small annular flow area and working pressure. In general, the gas leakage across pistons is small due
 321 to small diameters and low pressure variation [30]. The effect of gas leakage due to a typical radial
 322 clearance of $25\mu m$ [18] between the piston and cylinder wall is considered in Figure 7 for changing
 323 piston length. The gas leakage has almost no effect on the engine operation for piston lengths above
 324 3cm. However, for smaller clearance piston lengths the engine stroke decreases as a response to
 325 increasing gas leakage while the engine frequency is only slightly affected. Hence, we suggest no
 326 mechanical springs or special gas prevention techniques to be used. For large gas leakage, even the
 327 kinematic engine will stall and contact seals are recommended for engines with high gas leakage.



328

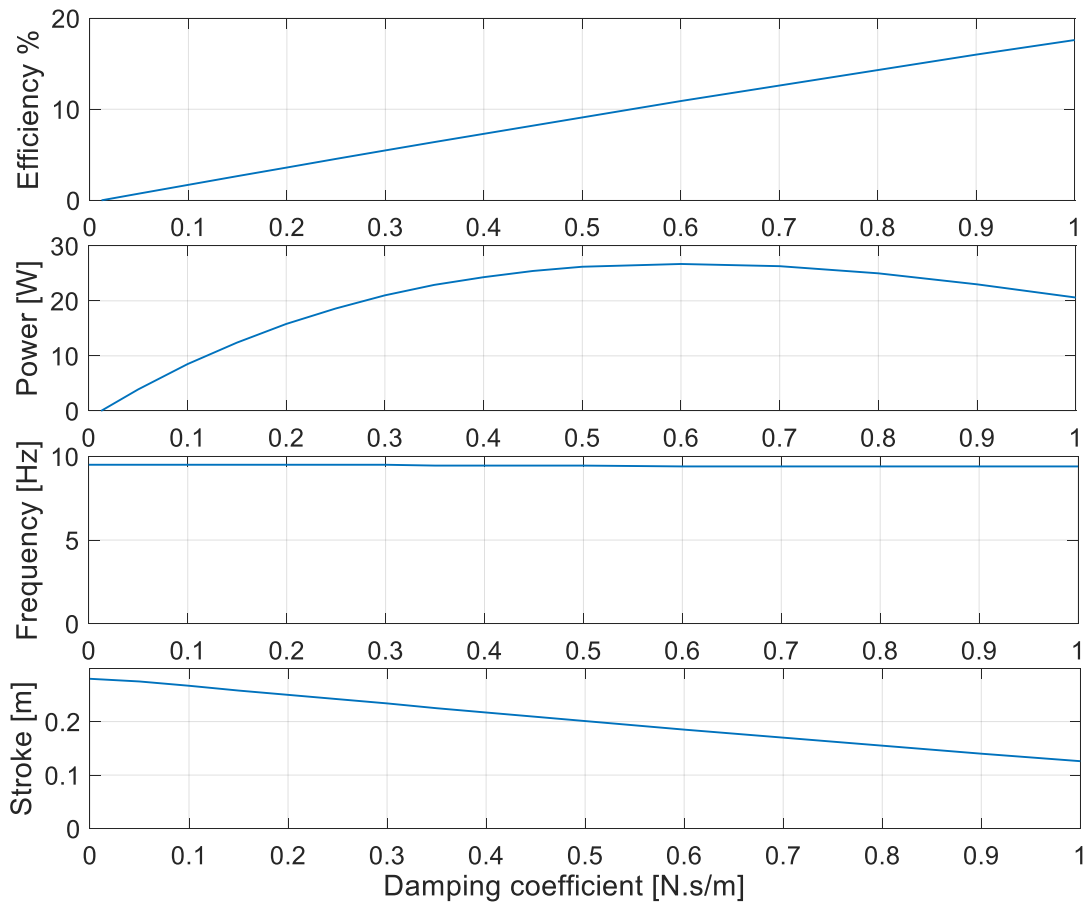
329 *Figure 7: Steady state response of the reference engine with changing clearance piston length L_g at no-load condition.*

330 **4.3 Loading the balanced compound engine**

331 In the kinematic engine, the engine stroke and piston instantaneous location are predetermined.
 332 Hence, the engine varies its speed as a response to the load. At no-load, the kinematic engine will
 333 accelerate until engine losses match the power generated and thus, the brake power is zero and
 334 engine speed is maximum. Loading the kinematic engine decreases its speed as well as the speed-
 335 accompanied losses. In contrast, the balanced compound engine has its speed determined by the
 336 stiffness of the gas spring and the reciprocator mass while its stroke is undetermined.

337 Figure 8 shows the effect of loading the 3-ph balanced compound engine by increasing the damping
 338 coefficient. The balanced compound Franchot engine has a slight frequency drop but a considerable
 339 stroke decrease as a response to increasing the load. Which make it suitable for fixed frequency
 340 applications like electricity generation. At no-load, the pistons reciprocate at the maximum stroke
 341 allowing heat to be transferred from the hot space to the cold space at highest rate without generating
 342 any useful power. At high engine loads, a stall point might be reached where no motion exists.
 343 Consequently, no heat will be exchanged and no power will be generated. Hence, a power maximum
 344 can be found in a point between the no-load and stall points while the efficiency is maximised as the
 345 load increases towards the stall point. The maximum power can be further maximised so that the
 346 stroke is slightly smaller than cylinder length but running the engine at no-load will cause the pistons
 347 to hit the walls. Hence, it is highly recommended that the engine must be designed at the no-load

348 condition unless the engine is always loaded. The phase angle is unaffected by the dynamic load and
 349 the engine is self-starting for various load values.

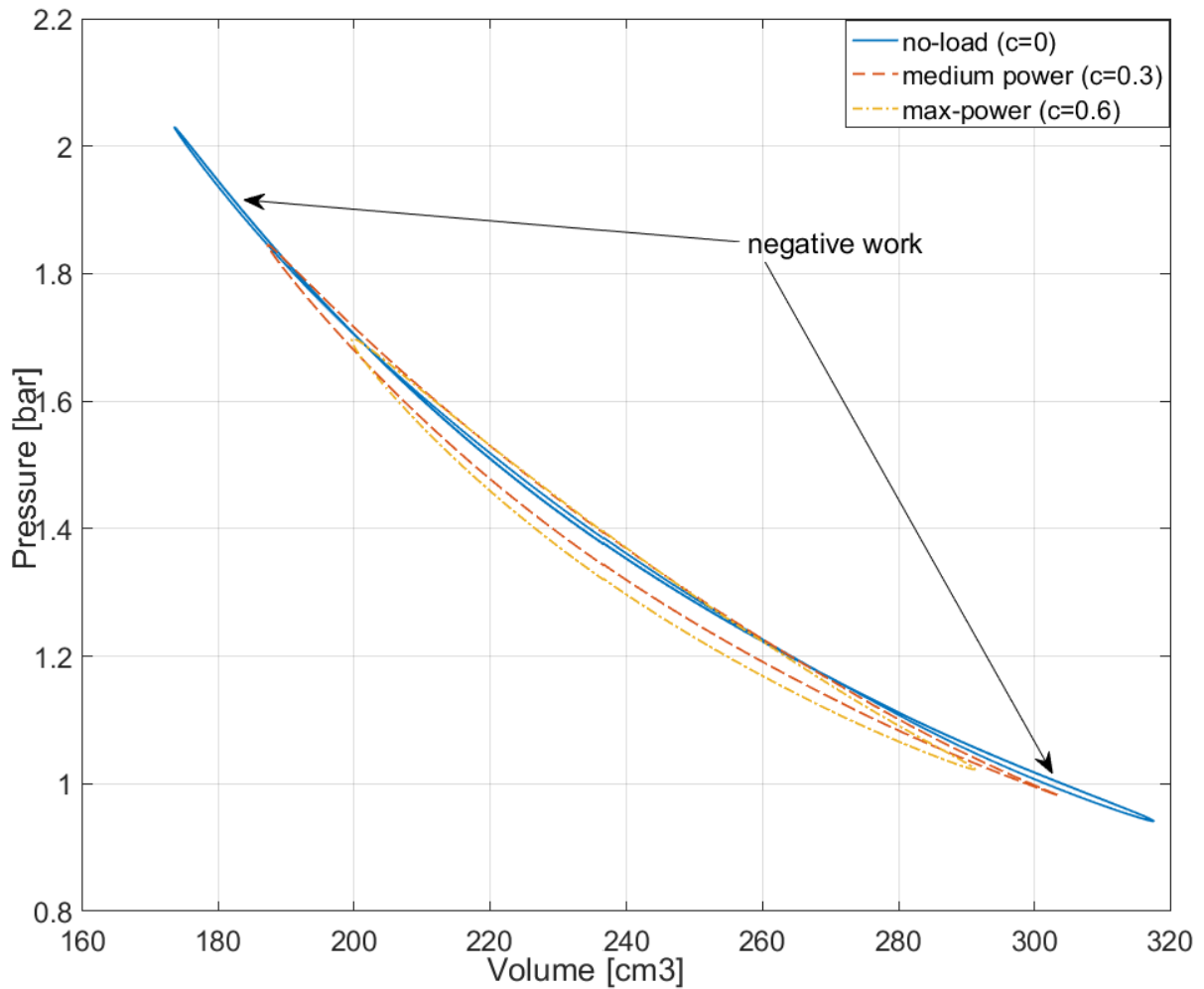


350

351 *Figure 8: Steady state response of the reference engine for changing the damping load.*

352 Figure 9 shows the PV diagram of the 3-ph balanced compound engine at the no-load, medium power
 353 and maximum power conditions. At the no-load condition, a butterfly shaped PV diagram shows two
 354 negative power regions where the compression overlaps with the expansion process and hence
 355 behaves like a gas spring [42]. This spring is important to the balanced compound engine to prevent
 356 the pistons from hitting the cylinder head by making gas cushions but it decreases the indicated work
 357 to zero at no-load. At medium and maximum powers, no negative work is found and both the pressure
 358 variation and swept volume are smaller than at the no-load case.

359



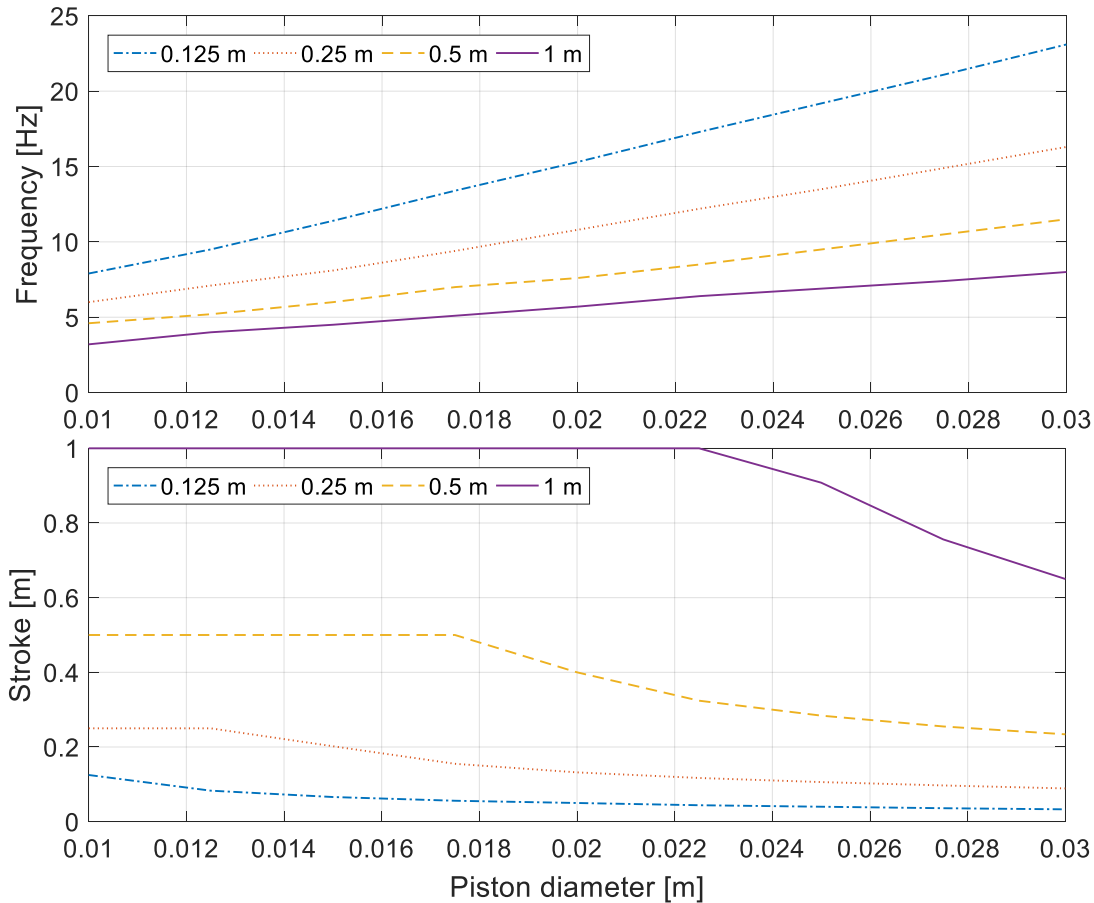
360

361 *Figure 9: PV diagram of the balanced compound engine at no-load and maximum power conditions.*

362

363 **4.4 Effect of geometry**

364 The geometry determines the resonant frequency, swept volume, heat transfer and piston forces
365 which all contribute in the performance of the balanced compound engine with heated and cooled
366 cylinders. The effect of increasing the engine cylinder diameters and lengths on the stroke and
367 frequency of the unloaded engine are shown in Figure 10. The increase in the diameter results in a
368 linear increase of the resonant frequency. Thus, a reduction of the engine stroke can be seen due to
369 the increase in the piston area so that the positive engine power matches with the negative power.

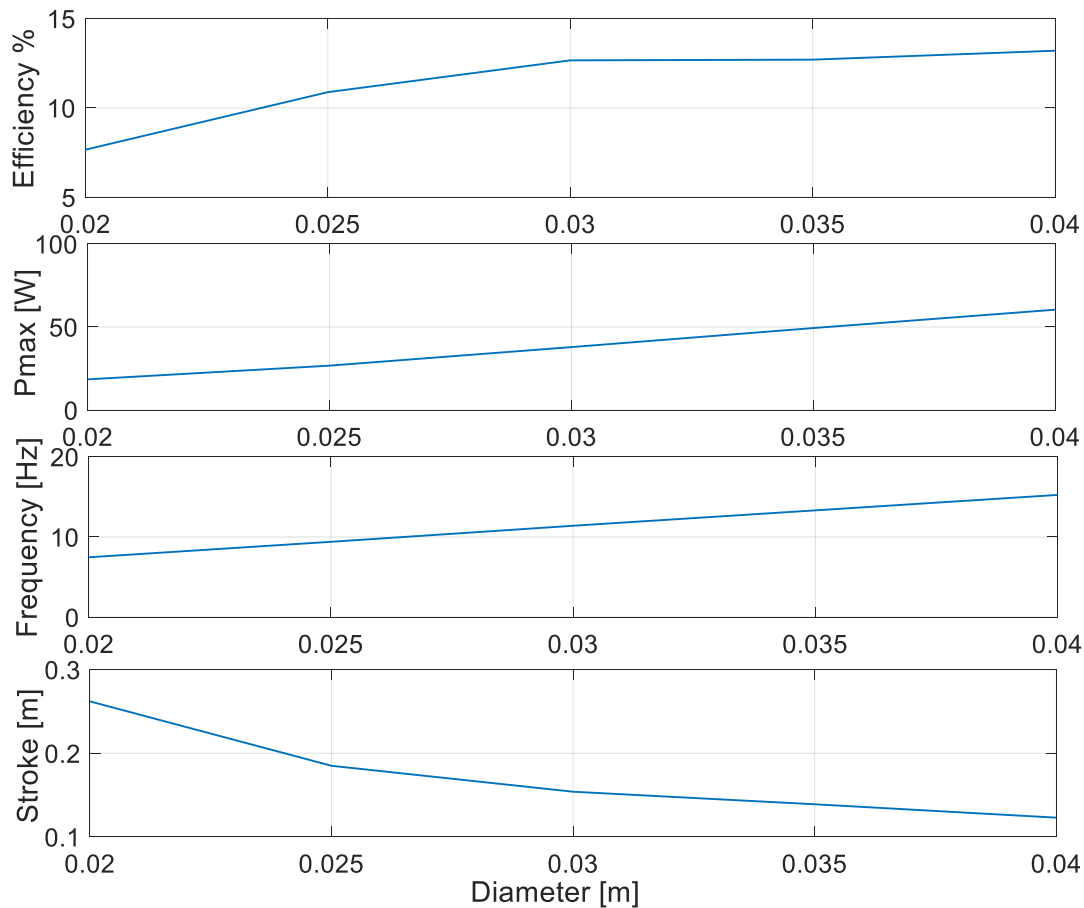


370

371 *Figure 10: Steady state response of the reference engine for changing engine diameter at no-load and for various cylinder*
 372 *lengths (0.125, 0.25, 0.5 and 1m).*

373 For long cylinders, the resonant frequency decreases as a result of reducing the working gas stiffness.
 374 In addition, longer cylinders also increase the heat transfer which in turn leads to longer strokes. It is
 375 found that the phase angle is kept unchanged with changing the cylinder geometry and the engine
 376 self-starts at no-load.

377 Figure 11 shows the influence of changing the diameter on the engine performance at the maximum
 378 power condition. It is found that increasing the diameter increases the maximum power and
 379 efficiency. The heat transfer increases due to increasing the Reynolds' number inside the engine
 380 cylinders which increases due to the diameter and the frequency of oscillation. The engine regulates
 381 itself by decreasing the stroke until maximising the power as a response to increasing the diameter.



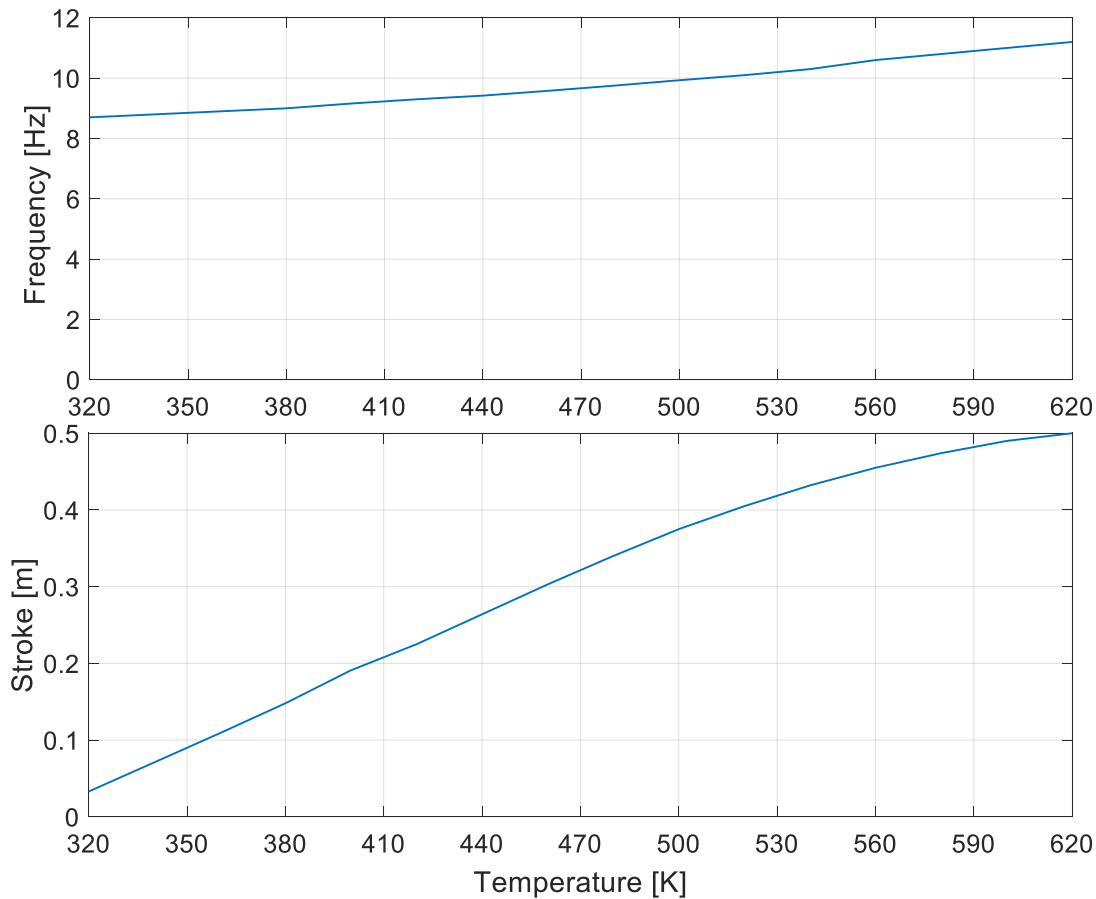
382

383 *Figure 11: Performance of the balanced compound Franchot engine at the maximum power with changing piston diameter.*

384 Large diameters generate large forces which help to overcome potential static mechanical frictions
 385 and loads hence ease the start-up of the balanced compound Franchot engine. Moreover, they
 386 prevent the pistons from hitting the cylinder especially at no-load condition.

387 **4.5 Effect of temperature**

388 The heat source temperature is the easiest parameter to control in the balanced compound engine
 389 and it has a major effect on engine power and efficiency. High temperature differences induce high-
 390 pressure variations and generate more cycle work than low temperatures. Thus both the frequency
 391 and stroke increase with increasing temperature differences as shown in Figure 12. The increase in
 392 the frequency can be attributed to the increase in the stiffness which is in turn increased as a response
 393 to the increased pressure variation. The phase angle is kept constant for changes in the temperature
 394 and the engine is self-starting for dynamic load. However, high temperature might cause the piston to
 395 hit the cylinder end plates. Hence, large temperatures require large diameters to decrease the stroke
 396 but this will also increase the frequency (see Figure 10). Alternatively, the engine load can be increased
 397 which will reduce the stroke without affecting the frequency and thus can prevent the piston hitting
 398 the cylinder end plates (see Figure 8). Accordingly, increasing the temperature can be used during the
 399 start-up to overcome the static friction.



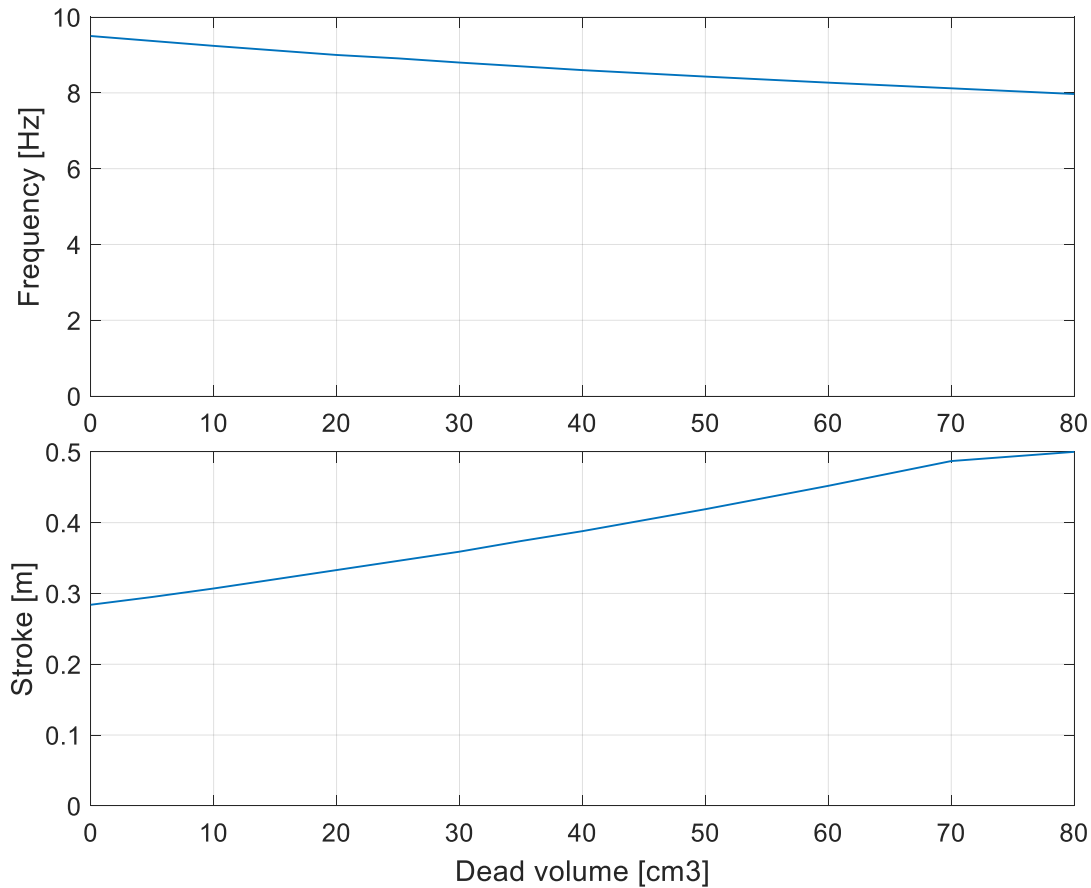
400

401 *Figure 12: Steady state response of the reference engine for changing hot cylinder temperatures and at no-load condition.*

402 **4.6 Effect of regenerator dead volume**

403 The dead volume increases the total engine volume, which reduces the gas stiffness and engine
 404 frequency. Moreover, an increased dead volume increases the engine thermal efficiency hence the
 405 engine stroke can increase. Thus, an increase in the stroke and decrease in the frequency is obtained
 406 for increasing the regenerator dead volume which can be seen in Figure 13.

407 At start-up, a large regenerator dead volume could prevent the pistons from moving due to the small
 408 pressure variation especially near the equilibrium point. Moreover, a large regenerator requires a long
 409 time to create a temperature gradient. Hence, an external kick-start or appropriate piston positioning
 410 might be required to start the motion. In addition, the dead volume can lead to the piston hitting the
 411 cylinder end plates hence causing an unstable operation but it can be optimised to maximise the
 412 power or enhance the efficiency. However, the self-starting capability and fixed phase angle is
 413 obtained for the 3-ph engine at no-load and dynamic load conditions for different regenerator
 414 volumes.



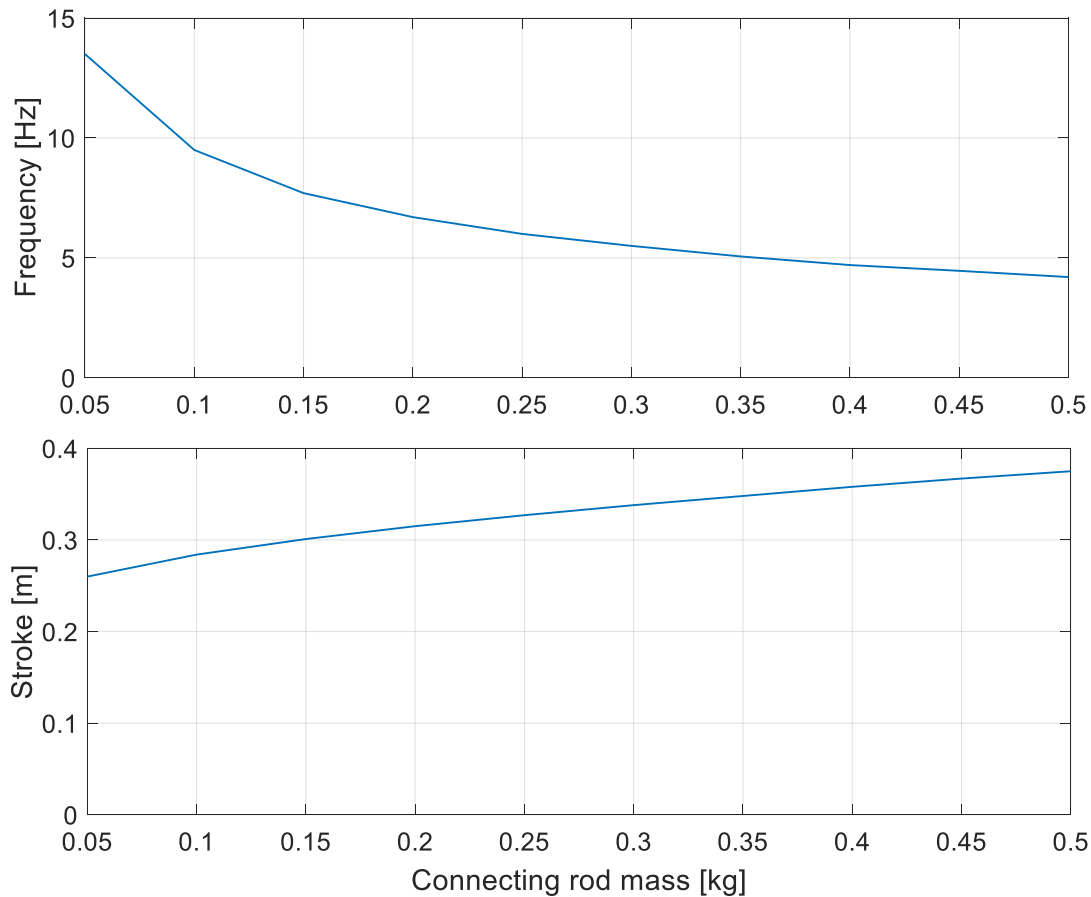
415

416 *Figure 13: Steady state response of the reference engine for changing regenerator dead volumes and at no-load condition.*

417 **4.7 Effect of reciprocator mass**

418 The mass should be as small as possible in ordered to have the lowest effect on the engine swept
 419 volumes, heat transfer and friction due to reciprocator weight. Reciprocating mass includes the
 420 pistons, connecting rods and the link between the connecting rods. Figure 14 shows that increasing
 421 the reciprocator mass causes the stroke to increase and frequency to decrease. Small masses increase
 422 the resonant frequency which behave similarly to increasing piston area. The self-starting capability
 423 and fixed phase angle is obtained for the 3-ph engine at the no-load condition with changing the mass
 424 of the reciprocator.

425



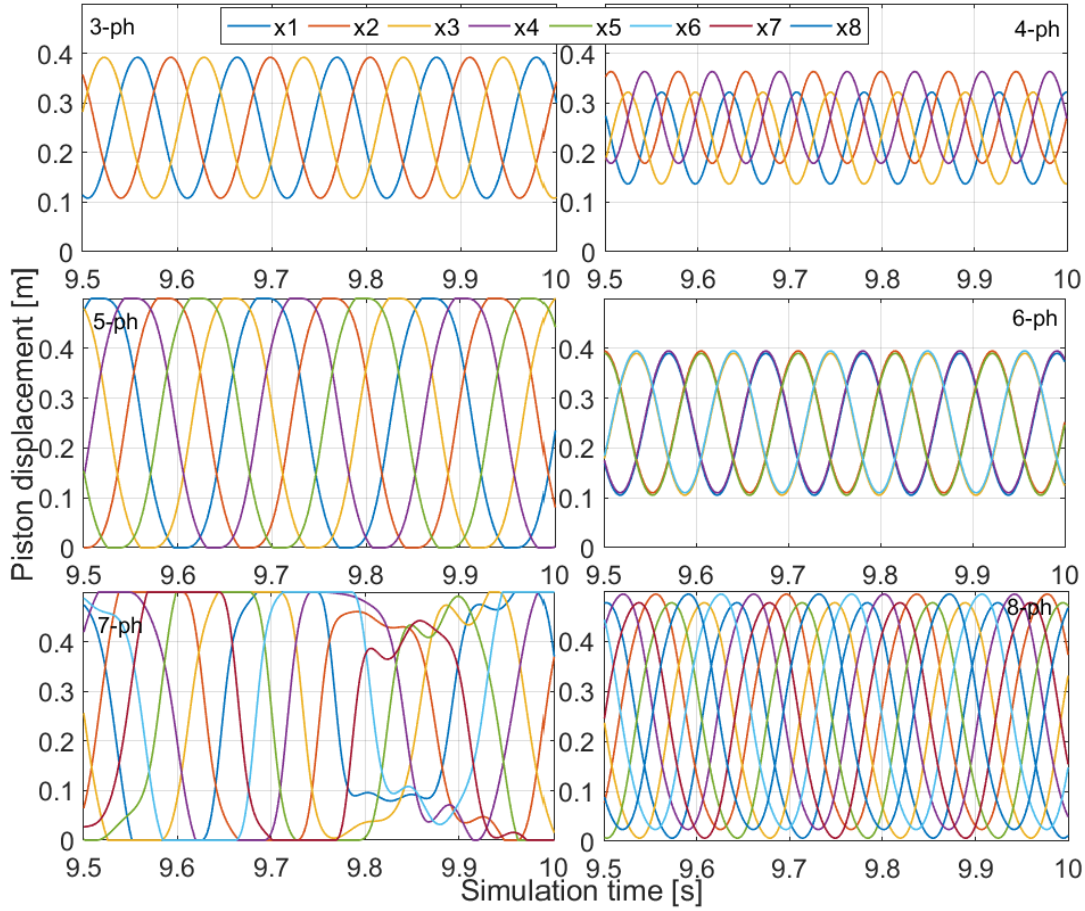
426

427 *Figure 14: Steady state response of the reference engine for changing reciprocator masses and at no-load condition.*

428

429 **4.8 Effect of number of cylinders**

430 The Franchot engine has the advantage of a flexible phase angle. For the balanced compound
 431 configuration, the phase angle is determined from the order of piston motion and regenerator
 432 connection. The number of cylinders is directly linked to the phase angle according to Table 1. The
 433 phase angle can be predicted for the 3-ph (six cylinders) and 4-ph (eight cylinders) Franchot engine
 434 since they have only single phase angles 120° and 90° respectively. In $n - ph$ Franchot engines where
 435 n is larger than four, the phase angle can take several values in the kinematic engine.



436

437 *Figure 15: No-load quasi steady state response for three to eight phase Franchot engine. The reciprocators' motion is given*
 438 *according to the displacement notation.*

439 Figure 15 shows that the $n - ph$ balanced compound Franchot engine always work on a single phase
 440 angle unlike the kinematic engine. The phase angle is determined from the lagging of a cold working
 441 volume of cylinder x_{i+1} to the neighbouring hot cylinder x_i because the regenerator connections are
 442 fixed. Hence, the motion sequence of the pistons in corresponding cylinders is used. Due to the even
 443 distribution of curves, the phase shift in a cycle is determined by dividing 360 by the number of
 444 distinguished phases. Following from this, the phase angle is calculated based on the number of phase
 445 shift peaks between the advancing and lagging curves x_i and x_{i+1} , respectively. For example, the 5 –
 446 ph engine has a phase shift of 72° due five phases and each cold space x_{i+1} lags the corresponding
 447 hot space x_i by two peaks which equals 144° . The 6-ph engine has only three distinguished phases
 448 which result in a phase shift of 60° and hence a phase angle of 120° due to only two peaks. Although
 449 small phase angles where anticipated for engines with large number of cylinders [20] the balanced
 450 compound Franchot engine operates always at the largest possible phase angle. At this phase angle,
 451 the pistons encounter the smallest possible piston forces due to the lower pressure difference
 452 compared to smaller phase angles. This means the balanced compound Franchot engine prefers the
 453 least resisting phase angle among the ones listed in Table 1. Thus, the phase angle of the balanced
 454 compound $n - ph$ Franchot engine can be written as:

$$\theta = \left\{ \begin{array}{ll} 180 - \frac{180}{n} & \text{for odd } n \\ 180 - \frac{360}{n} & \text{for even } n \end{array} \right\} \quad 35$$

455

456 The 4-ph Franchot engine has the smallest possible phase angle of 90° degree. This engine has the
457 shortest stroke and largest frequency because a small phase angle increases the pressure variation
458 which in turn increases the stiffness. Accordingly, the smallest frequency and the longest stroke can
459 be found at the largest phase angle where hitting the cylinder might occur. The 3-ph and 6-ph Franchot
460 engines have different number of cylinders but have nearly the same dynamic response due to having
461 the same phase angle. Large phase angle such as in the 7-ph engine have unsteady response. Due to
462 the large durations of hitting the wall, other pistons reciprocate creating pressure variations. However,
463 the impact with the wall consumes all the piston kinematic energy. Hence, hitting the wall must be
464 avoided for the engine longevity, durability, quietness and efficiency.

465 The odd phase balanced compound Franchot engines have similar phase angles and number of
466 cylinders to the multi-cylinder Siemens configuration but different phase shifts as two pistons are
467 moving together at the same time. The phase angle of the even phase Franchot engines lags behind
468 odd phase engines as the number of cylinders increases. The smallest possible number of cylinders is
469 3, 4 and 6 in the Siemens configuration, Finkelstein arrangement and balanced compound Franchot
470 engine, respectively.

471 **5 Conclusion**

472 The balanced compounding of the directly heated and cooled Franchot engine is mathematically
473 modelled and the engine response with respect to changes in friction, load, geometry, temperature,
474 dead volume and reciprocating mass has been discussed. The novel Franchot engine has a favourable
475 phase angle of 120° and short regenerator connections compared to the Finkelstein configuration.
476 The friction created by side forces can be decreased by increasing the length of the engine and by
477 decreasing the offset between the cylinders. The engine is self-starting because the friction prevents
478 the engine from stopping exactly at mid stroke. Thus, the engine has great potential as a prime mover
479 for liquid or heat pumps or electric generators.

480 Due to the absence of the crankshaft, the balanced compound Franchot engine can have incomplete
481 strokes but with a fixed phase angle and nearly constant frequency as a response to increasing load.
482 The performance of the free piston engine depends on the geometry, temperatures, dead volume,
483 reciprocator mass, number of cylinders and load. Small loads, high temperatures, large dead volumes
484 and low diameters increase the stroke which might lead to the pistons hitting the cylinder heads.

485 The dynamic model of the balanced compound Franchot engine confirms the potential phase angles
486 that were found using the instantaneous power method for the 3-ph and 4-ph Franchot engines which
487 equals the phase shift. In addition, it is shown that the $n - ph$ balanced compound Franchot engine
488 always prefers the largest possible phase angle so that it operates with the least resisting loads.

489 In the balanced compounding, the Franchot engine can have only a single phase angle which limits its
490 advantages. However, the phase angle can be adjusted by changing the number of cylinders. The
491 simplest form of the $n - ph$ free piston engine is the 3-ph engine. It has the shortest regenerator
492 connections, smallest number of cylinders, a favourable phase angle and it has potential for electricity
493 generation. In contrast to the Finkelstein configuration, the side-by-side balanced compound 3-ph
494 engine has a 120° phase angle, shorter regenerator connections and long engine strokes but it could
495 not eliminate the side forces on the connecting rods. The balanced compound engine is suggested for
496 pumping and power generation applications as its response has nearly constant frequency with the
497 load.

498 **Acknowledgement**

499 The authors would like to thank the British Council - HESPAL for the Ph.D scholarship for Jafar M.
500 Daoud.

501 References

- 502 [1] G. Walker, "Coal-fired Stirling engines for railway locomotive and stationary power
503 applications," *Proc Instn Mech Engrs*, vol. 197A, no. October, pp. 233–246, 1983.
- 504 [2] M. H. Ahmadi, H. Sayyaadi, S. Dehghani, and H. Hosseinzade, "Designing a solar powered
505 Stirling heat engine based on multiple criteria: Maximized thermal efficiency and power,"
506 *Energy Convers. Manag.*, vol. 75, pp. 282–291, Nov. 2013.
- 507 [3] S. Toghyani, A. Kasaeian, and M. H. Ahmadi, "Multi-objective optimization of Stirling engine
508 using non-ideal adiabatic method," *Energy Convers. Manag.*, vol. 80, pp. 54–62, Apr. 2014.
- 509 [4] M. H. Ahmadi, M. A. Ahmadi, A. Mellit, F. Pourfayaz, and M. Feidt, "Thermodynamic analysis
510 and multi objective optimization of performance of solar dish Stirling engine by the centrality
511 of entransy and entropy generation," *Int. J. Electr. Power Energy Syst.*, vol. 78, pp. 88–95, Jun.
512 2016.
- 513 [5] B. Hoegel, D. Pons, M. Gschwendtner, and A. Tucker, "Theoretical investigation of the
514 performance of an Alpha Stirling engine for low temperature applications," *ISEC Int. Stirling
515 Engine Comm.*, no. January, 2012.
- 516 [6] T. Finkelstein, "Optimization of phase angle and volume ratio for Stirling engines," Jan. 1960.
- 517 [7] M. H. Ahmadi, M.-A. Ahmadi, and F. Pourfayaz, "Thermal models for analysis of performance
518 of Stirling engine: A review," *Renew. Sustain. Energy Rev.*, vol. 68, no. October 2016, pp. 168–
519 184, 2017.
- 520 [8] N. W. Lane and W. T. Beale, "Free-piston Stirling design features," *Eighth International Stirling
521 Engine Conference*. 1997.
- 522 [9] G. Fenies, F. Formosa, J. Ramousse, and A. Badel, "Double acting Stirling engine: Modeling,
523 experiments and optimization," *Appl. Energy*, vol. 159, pp. 350–361, 2015.
- 524 [10] E. D. Rogdakis, N. A. Bormpilas, and I. K. Koniakos, "A thermodynamic study for the
525 optimization of stable operation of free piston Stirling engines," *Energy Convers. Manag.*, vol.
526 45, no. 4, pp. 575–593, 2004.
- 527 [11] W. T. Beale, "Free Piston Stirling Engines - Some Model Tests and Simulations," 1969, pp. 1–
528 10.
- 529 [12] W. T. BEALE, "Stirling cycle type thermal device," U.S. Patent 3,552,120, 1971.
- 530 [13] A. Der Minassians and S. R. Sanders, "Multiphase Stirling Engines," *J. Sol. Energy Eng.*, vol. 131,
531 no. 2, p. 21013, 2009.
- 532 [14] G. Walker and J. R. Senft, *Free Piston Stirling Engines*, First edit., vol. 12. Berlin, Heidelberg:
533 Springer Berlin Heidelberg, 1985.
- 534 [15] M. A. White, J. E. Augenblick, and A. A. Peterson, "Double acting thermodynamically resonant
535 free-piston multicylinder Stirling system and method," U.S. Patent 7,134,279 B2, 2006.
- 536 [16] W. T. Beale, "Pressure modulation system for load matching and stroke limitation of Stirling
537 cycle apparatus," U.S. Patent 4,458,495, 1984.
- 538 [17] D. G. Thombare and S. K. Verma, "Technological development in the Stirling cycle engines,"
539 *Renew. Sustain. Energy Rev.*, vol. 12, no. 1, pp. 1–38, Jan. 2008.

- 540 [18] B. Hoegel, "Thermodynamics-based design of stirling engines for low-temperature heat
541 sources.," University of Canterbury, 2014.
- 542 [19] D. M. Berchowitz and Y.-R. Kwon, "Multiple Cylinder Free-Piston Stirling Machinery," *J. Power
543 Energy Syst.*, vol. 2, no. 5, pp. 1209–1220, 2008.
- 544 [20] D. M. Berchowitz and Y.-R. KWon, "Multiple-cylinder, free-piston, alpha configured Stirling
545 engines and heat pumps with stepped pistons," U.S. Patent 7,171,811 B1, 2007.
- 546 [21] A. Der Minassians, "Stirling Engines for Low-Temperature Solar-Thermal- Electric Power
547 Generation," University of California at Berkeley, 2007.
- 548 [22] C. D. West, "Liquid-piston Stirling machines," in *2nd International Conference on Stirling
549 engines*, 1984, pp. 15–36.
- 550 [23] J. W. Mason and J. W. Stevens, "Characterization of a solar-powered fluidyne test bed,"
551 *Sustain. Energy Technol. Assessments*, vol. 8, pp. 1–8, 2014.
- 552 [24] T. Finkelstein, "balanced compounding of Stirling machines," in *Intersociety Energy Conversion
553 Engineering Conference, 13th*, 1978, pp. 1791–1797.
- 554 [25] T. Finkelstein, "Method and device for balanced compounding of Stirling cycle machines," U.S.
555 Patent 4,199,945, 1980.
- 556 [26] T. Finkelstein, "Analysis of Heat-Activated Stirling Heat Pump," in *Intersociety Energy
557 Conversion Engineering Conference*, 1980, pp. 1788–1796.
- 558 [27] T. Finkelstein, "Isothermal Sinusoidal Analysis of Balanced Compound Vuilleumier Heat
559 Pumps," in *27th Intersociety Energy Conversion Engineering Conference (1992)*, 1992.
- 560 [28] Robert F. McConaghy, "Multi-cylinder free piston Stirling engine," U.S. Patent 0,193,266 A1,
561 2007.
- 562 [29] M. W. Dadd, "Linear Multi-cylinder Stirling Cycle Machine," U.S. Patent 8,820,068 B2, 2014.
- 563 [30] J. M. Daoud and D. Friedrich, "Performance investigation of a novel Franchot engine design,"
564 *Int. J. Energy Res.*, Aug. 2017.
- 565 [31] J. M. Daoud and D. Friedrich, "Parametric Study of an Air Charged Franchot Engine with Novel
566 Hot and Cold Isothermalizers," *Inventions*, vol. 2, no. 4, p. 35, Dec. 2017.
- 567 [32] J. M. Daoud and D. Friedrich, "A novel Franchot engine design based on the balanced
568 compounding method," *J. Mech. Sci. Technol.*, vol. under revi.
- 569 [33] S. Chatterton and P. Pennacchi, "Design of a Novel Multicylinder Stirling Engine," *J. Mech. Des.*,
570 vol. 137, no. 4, p. 42303, 2015.
- 571 [34] H. Karabulut, "Dynamic analysis of a free piston Stirling engine working with closed and open
572 thermodynamic cycles," *Renew. Energy*, vol. 36, no. 6, pp. 1704–1709, 2011.
- 573 [35] R. W. Redlich and D. M. Berchowitz, "Linear Dynamics of Free-Piston Stirling Engines," *Proc.
574 Inst. Mech. Eng. Part A Power Process Eng.*, vol. 199, no. 3, pp. 203–213, Aug. 1985.
- 575 [36] K. Hirata, "A10 Development of 2-cylinder Double-Acting Stirling Engine," in *The Proceedings
576 of the Symposium on Stirling Cycle*, 2006, vol. 2006.10, pp. 93–96.
- 577 [37] S.-Y. Kim and D. Berchowitz, "Specific Power Estimations for Free-Piston Stirling Engines," in
578 *4th International Energy Conversion Engineering Conference and Exhibit (IECEC)*, 2006, no.
579 June.

- 580 [38] M. Babaelahi and H. Sayyaadi, "Modified PSVL: A second order model for thermal simulation
581 of Stirling engines based on convective-polytropic heat transfer of working spaces," *Appl.*
582 *Therm. Eng.*, vol. 85, pp. 340–355, 2015.
- 583 [39] R. Li, L. Grosu, and D. Queiros-condé, "Losses effect on the performance of a Gamma type
584 Stirling engine," *Energy Convers. Manag.*, vol. 114, pp. 28–37, 2016.
- 585 [40] M. Costea and M. Feidt, "The effect of the overall heat transfer coefficient variation on the
586 optimal distribution of the heat transfer surface conductance or area in a Stirling engine,"
587 *Energy Convers. Manag.*, vol. 39, no. 16–18, pp. 1753–1761, Nov. 1998.
- 588 [41] F. Toda, S. Iwamoto, M. Matsuo, and Y. Umezane, "Heat Transfer on a Small Stirling Engine," *J.*
589 *Mar. Eng. Soc. JAPAN*, vol. 25, no. 6, pp. 358–365, 1990.
- 590 [42] C. Fernández-Aballí-Altamirano, M. Calcoen, E. Vandermeersch, and J. J. González-Bayón,
591 "Experimental Tailer like Thermal Lag Engine to obtain pressure and volume diagrams," *Ing.*
592 *Mecánica*, vol. 16, no. 1, pp. 35–40, 2013.
- 593